



**Discussion Papers  
in Economics**

**No. 04/2017**

## **A General Class of Entropy Based Control Charts**

**Benedikt Mangold**  
University of Erlangen-Nürnberg

**Jens Konopik**  
University of Erlangen-Nürnberg

ISSN 1867-6707

# A General Class of Entropy Based Control Charts

Benedikt Mangold<sup>a,1</sup>, Jens Konopik<sup>a</sup>

<sup>a</sup>*University of Erlangen-Nürnberg, Department of Statistics and Econometrics, Lange Gasse 20,  
90403 Nürnberg, Germany*

Wednesday 1<sup>st</sup> February, 2017

---

## Abstract

We introduce a new class of Shewhart control charts, namely the  $\phi$ -chart. This new class is based on the cumulative paired  $\phi$ -divergence that generalizes both the cumulative (residual) entropy and the differential entropy. The  $\phi$ -chart contains several subclasses; of which one has as a special case the  $G$ -chart, which uses Gini's mean difference as a measure of dispersion. We investigate the performance of three of the subclasses of  $\phi$ -charts in a showcase scenario, comparing its average run length under the Gaussian and several alternative distributions. We find especially the new Leik control chart to outperform classical Shewhart charts, which are based on ranks, standard deviation, or Gini's mean difference. Monitoring a production process using  $\phi$ -charts implies a faster detection of an out-of-control process, which can be crucial for a variety of application areas.

*Keywords:* Control chart, entropy, Gini's mean difference, cumulative paired  $\phi$ -entropy

---

---

*Email addresses:* [benedikt.mangold@fau.de](mailto:benedikt.mangold@fau.de) (Benedikt Mangold), [jens.konopik@fau.de](mailto:jens.konopik@fau.de) (Jens Konopik)

<sup>1</sup>The authors have benefited from many helpful discussions with Monika Doll

## 1. Introduction

Shewhart control charts are an essential tool for quality control in the context of supervising processes of production. These charts, introduced by [Shewhart \(1931\)](#), are essentially based on interpretation of mean, standard deviation, and range of samples obtained from production processes.

Control charts try to determine whether processes are still under control. A classical example is the  $\bar{x}S$ -chart, which assumes that the quantity that is to be controlled follows a normal distribution. In this case, the  $\bar{x}$ -chart monitors the process mean and checks whether the controlled sample values lie between two acceptance boundaries. Additionally, the  $S$ -chart checks if the  $\bar{x}$ -chart's boundaries are still represented by the variance of the monitored process and shows off limits in which the process variance can vary without being classified as *changed*. Here,  $S$  is the sample standard deviation, defined as

$$S = \sqrt{\sum_{i=1}^n (X_i - \bar{X})^2 / (n - 1)}.$$

[Burr \(1967\)](#) analysed the suitability of  $\bar{x}$ -chart's boundaries for samples drawn from non-normal parent populations. His results showed that the usual boundaries are still reliable if the sample's distribution does not deviate too much from the normal distribution. In line with this results, [Chan et al. \(1988\)](#) concluded that charts, which are designed for normal distributed data, do not work well if the underlying distribution has extremely heavy or light tails.

Next to this, [Page \(1954\)](#) and [Ewan \(1963\)](#) used a cumulative sum and [Crowder \(1987\)](#) an exponentially weighted moving average to supervise production processes and demonstrated these methods' advantages in case of small changes in the nature of the process.

Recent research by [Riaz and Saghir \(2007\)](#) as well as [Saghir and Lin \(2015\)](#) employed Gini's mean difference for tracing the variability of production processes. They carved out situations in which a  $G$ -chart<sup>2</sup> is able to more efficiently detect changes in the variance of a process than charts that are currently applied in supervision, like the previously explained, especially in situations, in which the data's distribution is not normal.

---

<sup>2</sup>The  $G$ -chart is a control chart based on Gini's mean difference.

We introduce a new class of control charts, the  $\phi$ -chart, which is a generalization based on a new class of entropy, the cumulative paired  $\phi$ -entropy ( $CPE_\phi$ ) as introduced by Klein et al. (2016). The  $CPE_\phi$  contains many classes of well-known entropies such as the cumulative (residual) entropy and the differential entropy. We generalize the results of Riaz and Saghir (2007) and Saghir and Lin (2015) as follows: First, a class of  $\phi$ -charts is introduced that inherits the  $G$ -chart as a special case. Second, two new control charts are introduced that can be of advantageous use as a control chart in situations, in which a sample of the process is not drawn from a normal population.

This paper is organized as follows: At the beginning, we introduce the  $G$ -chart by Riaz and Saghir (2007) and Saghir and Lin (2015). Then we introduce the new class of  $\phi$ -charts<sup>3</sup>. Section 3 compares the  $\phi$ -charts to the established  $S$ - and  $G$ -charts in a showcase scenario. Section 4 summarizes and discusses our findings.

## 2. Methodology

Throughout this paper, we analyse methods to monitor the variability of a process. Information about location is not focus of this research. Therefore, we assume in the following that any sample mean values lie in their control limits, meaning process location is under control.

Control limits for the variability of a sample with  $n$  observations are defined as

$$\begin{aligned} \text{Lower Control Limit, LCL} &= \sigma q_{\frac{\alpha}{2},n} \\ \text{Upper Control Limit, UCL} &= \sigma q_{1-\frac{\alpha}{2},n}. \end{aligned}$$

If the populations standard deviation  $\sigma$  is unknown, it can be replaced by an unbiased estimator  $\hat{\sigma}$  in the case of a normal distribution. The quantiles  $q_\alpha$  are obtained from a Monte Carlo simulation, since exact distributions can be difficult to determine for finite  $n$ <sup>4</sup>.

---

<sup>3</sup>Note, that we will not provide an analysis with respect to the  $R$ -chart, which is based on ranks of a sample. This decision is based on the finding of Riaz and Saghir (2007), who showed that the  $R$ -chart is either dominated by one, the  $S$ - or the  $G$ -chart.

<sup>4</sup>See Riaz and Saghir (2007) for further details on the critical values for  $S$ - and  $G$ -charts under normality.

## 2.1. $G$ -chart

A  $G$ -chart is based on Gini's mean difference measure:

$$G = \frac{2}{n(n-1)} \left( \sum_{\substack{i=1 \\ i \neq j}}^n \sum_{j=1}^n |x_i - x_j| \right).$$

David (1968) showed, that  $(\sqrt{\pi}/2)G$  is an unbiased estimator for the true underlying process variability. Saghir and Lin (2015) analyzed the performance of  $G$ -charts under several violations of assumptions as non-normality and shifts in the standard deviation of the process.

## 2.2. $\phi$ -charts

Klein et al. (2016) introduced a new kind of entropy whose special cases have been used in a variety of fields of research, such as Fuzzy set theory (c.f. de Luca and Termini (1972)), Uncertainty theory (c.f. Liu (2015)), and Reliability theory (c.f. Ebrahimi (1996)). This new class of entropy, cumulative paired  $\phi$ -entropy ( $CPE_\phi$ ), is based on an absolute continuous probability distribution function  $F$ . For every concave function  $\phi$  with  $\phi(0) = \phi(1) = 0$ , the  $CPE_\phi$  is defined as

$$CPE_\phi(F) = \int_{\mathbb{R}} \phi(F(x)) + \phi(1 - F(x)) dx.$$

$\phi$  is called entropy generating function. Next, we use the following four  $CPE_\phi$  as measures of variability resulting in four  $\phi$ -charts:

1. Cumulative paired Leik entropy ( $CPE_L$ , following Leik (1966)) is generated by

$$\phi(u) = \min\{u, 1 - u\} = \frac{1}{2} - \left| u - \frac{1}{2} \right|, \quad u \in [0, 1],$$

which results in

$$CPE_L(F) = 2 \int_{\mathbb{R}} \min\{F(x), 1 - F(x)\} dx.$$

2. Cumulative paired  $\alpha$ -entropy ( $CPE_\alpha$ , following Havrda and Charvát (1967)) is generated by

$$\phi(u) = u \frac{u^{\alpha-1} - 1}{1 - \alpha}, \quad u \in [0, 1] \text{ and } \alpha > 1,$$

which results in

$$CPE_\alpha(F) = \int_{\mathbb{R}} \left( F(x) \frac{F(x)^{\alpha-1} - 1}{1 - \alpha} + (1 - F(x)) \frac{(1 - F(x))^{\alpha-1} - 1}{1 - \alpha} \right) dx.$$

3. Cumulative paired Shannon entropy ( $CPE_S$ , following [Burbea and Rao \(1982\)](#)) is generated by

$$\phi(u) = -u \ln u, \quad u \in [0, 1],$$

which results in

$$CPE_S(F) = - \int_{\mathbb{R}} (F(x) \ln F(x) + (1 - F(x)) \ln(1 - F(x))) dx.$$

The  $CPE_S$  is a special case of  $CPE_\alpha$  for  $\alpha \rightarrow 1$ .

4. Cumulative paired Gini entropy ( $CPE_G$ ), which is a special case of  $CPE_\alpha$  for  $\alpha = 2$ , results in

$$CPE_G(F) = 2 \int_{\mathbb{R}} F(x)(1 - F(x)) dx.$$

Note, that since  $G = 4CPE_\phi$ ,  $G$ -charts can be generalized to  $\alpha$ -charts or even more general  $\phi$ -charts, that contain the  $G$ -chart as a special case. See [Klein et al. \(2016\)](#) for information about the estimation of  $CPE_\phi$ .

We compare this generalizations to the established results in literature in the next section.

### 3. Results

Following [Riaz and Saghir \(2007\)](#) and [Saghir and Lin \(2015\)](#), we evaluate the charts' performance via a simulation study. For simulating quantiles that are required for the control limit, we use a Monte Carlo simulation with 2,000,000 random samples of size  $n = 6$  and a significance level of 1% as reference case. Table 1 gives an overview on the probability distributions used throughout the simulation. For the Normal, logistic, Laplace, and exponential distribution, a standardizing parametrization is used. We choose  $\nu = 5$  degrees of freedom for the Student  $t$  distribution for modelling heavy tails, while ensuring the existence of the first four moments.

| Distribution | Density function   | Parameters                   |
|--------------|--|------------------------------|
| Normal       | $\frac{1}{\sqrt{2\pi\sigma^2}} \exp\left(-\frac{(x-\mu)^2}{2\sigma^2}\right)$  | $\mu = 0, \sigma = 1$        |
| Student $t$  | $\frac{\Gamma(\frac{\nu+1}{2})}{\sqrt{\nu\pi}\Gamma(\frac{\nu}{2})} \left(1 + \frac{x^2}{\nu}\right)^{-\frac{\nu+1}{2}}$ | $\nu = 5$                    |
| Logistic     | $\frac{\exp\left(-\frac{x-\mu}{\sigma}\right)}{\sigma\left(1+\exp\left(\frac{x-\mu}{\sigma}\right)\right)^2}$            | $\mu = 0, \sigma = 1$        |
| Gamma        | $\frac{1}{\Gamma(\tau)\theta^\tau} x^{\tau-1} \exp\left(-\frac{x}{\theta}\right)$  | $\tau \geq 0, \theta \geq 0$ |
| Laplace      | $\frac{1}{2b} \exp\left(-\frac{ x-\mu }{b}\right)$   | $\mu = 0, b = 1$             |
| Exponential  | $\lambda \exp(-\lambda x)$   | $\lambda = 1$                |

Table 1: Density functions of the analyzed probability distributions.

### 3.1. Evaluation metric

Following [Saghir and Lin \(2015\)](#), we use the average run length ( $ARL$ ) as performance criterion for the suitability of the proposed charts in several scenarios. The  $ARL$  is defined as  $\frac{1}{1-\beta}$ , hence a transformation of the testing procedure's power. It can be interpreted as the average required amount of observations from the process until a out-of-control situation is detected. We distinguish between  $ARL_0$  (run length when a process is under control) and  $ARL_1$  (run length when a process is not under control). For a suitable chart,  $ARL_0$  has to be large – since an alarm would be a wrong decision – and  $ARL_1$  has to be small – to detect out-of-control situations as quickly as possible. The  $ARL$  values that are displayed in the following are the result of a Monte Carlo experiment with 200,000 repetitions.

The reference standard deviation  $\sigma$  for each distribution is defined by the corresponding parameters in table 1. The violation of the process' assumptions is implemented by shifting the reference standard deviation for each distribution from  $\sigma$  to  $k\sigma$  with  $k > 1$ . Furthermore we change the actual distribution of the process, implemented by using one of the other 5 distributions from table 1 instead of the Gaussian distribution.

### 3.2. Performance of $\phi$ -charts

#### $\alpha$ -charts for $\alpha \neq 2$

First, we are interested in analyzing the close surrounding of the special case  $\alpha = 2$ . We compared  $ARL_0$  and  $ARL_1$ . As it turns out, there is no relevant improvement in neither  $ARL_0$  or  $ARL_1$  from using the  $G$ -chart<sup>5</sup> to any value  $\alpha \neq 2$ , neither if the variance increases while the distribution remains Gaussian nor if other distributions from table 1 are applied. Figure 1 illustrates this finding exemplarily by showing the standardized  $ARL_0$  (left) and  $ARL_1$  values (right) of the  $\alpha$ -charts (including the  $G$ -chart) as ratio with respect to the  $ARL_0$  and  $ARL_1$  values of the  $S$ -charts – for different values of  $\alpha$ , for the Gaussian and the exponential distribution.

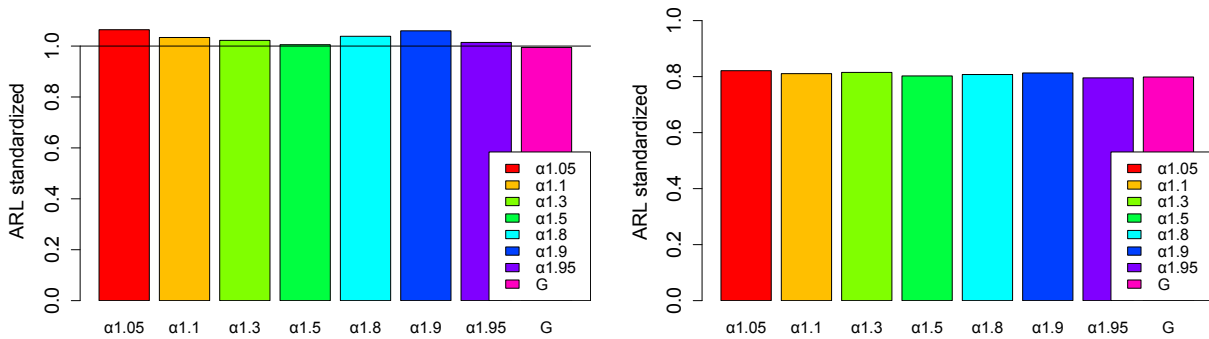


Figure 1: Ratios of  $ARL$  of  $\alpha$ -charts for  $1 < \alpha < 2$  and the  $ARL$  of  $S$ . Left:  $ARL_0$  for standard Gaussian data. Right:  $ARL_1$  of sample from exponential distribution with  $\lambda = 0.625$ .

We see that figure 1 shows nearly no difference between the performance of  $\alpha$ -charts and the  $S$ -charts for any value of  $\alpha \in (1, 2]$ . This seems to be surprising at first sight – a closer look at the entropy generating function  $\phi$  clarifies this finding. All functions weight data points in a similar manner, the more they are located in the tails of a distribution. Since those observations are responsible for tremendous changes in variability, the detection of out-of-control situations by  $\alpha$ -charts for any value of  $\alpha$  is similar. The functional form of the  $CPE_\phi$ 's integrand  $\phi(u) + \phi(1 - u)$  for different values of  $\alpha$  is displayed in figure 2. As

<sup>5</sup>The  $G$ -chart is an  $\alpha$ -chart with  $\alpha = 2$



we will see in the following section, more advantageous behavior of a  $\phi$ -chart can only be expected if the shape of  $\phi(u) + \phi(1-u)$  varies considerably, as with the Leik-chart.

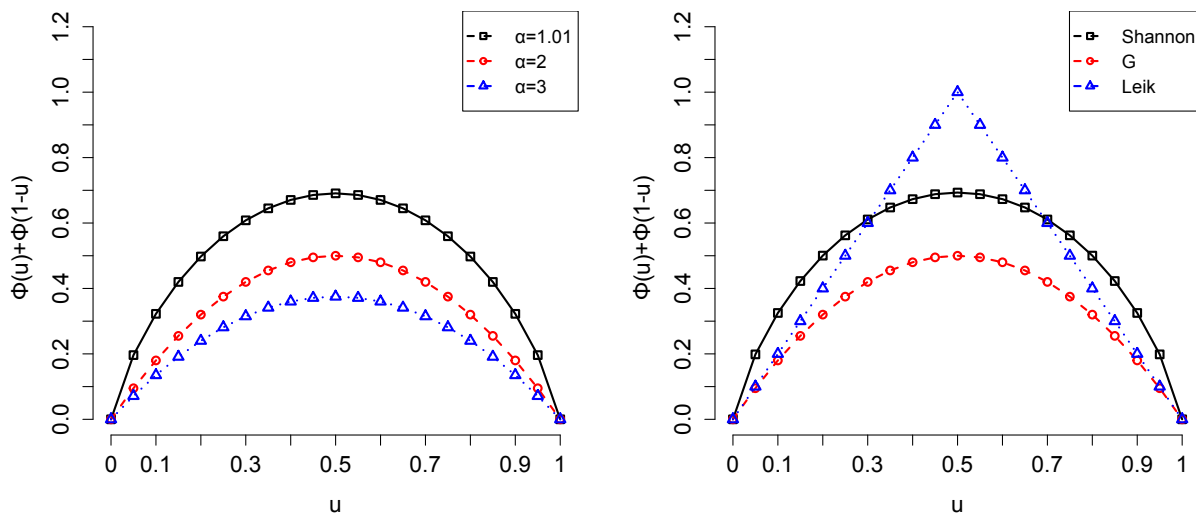


Figure 2: The integrands of:  $CPE_\alpha$  for  $\alpha = 1.01, 2, 3$  (left); The integrands of:  $CPE_G$ ,  $CPE_S$ , and  $CPE_L$  (right).

### Shannon- and Leik-charts

In this section we analyze the  $ARL$  of charts that are based on the Leik entropy  $CPE_L$  as well as on the Shannon entropy  $CPE_S$ . As can be seen from figure 2, the integrands of the resulting  $CPE_\phi$  have substantially different slopes in the tail regions. In the following, we take a closer look on how this affects the  $ARL$  of the associated  $\phi$ -charts. We use the Shannon-chart and the  $G$ -chart as representatives of the  $\alpha$ -charts, since the previous section showed very similar behaviour referring different values of  $\alpha$ .

At first we evaluate the Leik- and Shannon-chart in the default setting, shifting the standard deviation of a Gaussian distribution. Figure 3 summarizes the  $ARL$ -values of  $G$ -charts in comparison to Shannon- and Leik-charts. All values are displayed relative to the respective  $ARL$  of the benchmarking  $S$ -chart. Results show that neither of the new  $\phi$ -charts outperforms the  $S$ -chart in the sense of a higher  $ARL_0$  or a lower  $ARL_1$ . However, the  $ARL_0$  of the  $G$ -, Leik-, and Shannon-charts are not significantly different from values of the  $S$ -chart. All  $ARL_1$  values converge as the multiplicative shift  $k$  of the standard deviation increases. However, the Leik-chart has difficulties detecting smaller shifts around  $k \in (1, 2]$ . In contrast to the  $S$ -chart, the Leik-chart needs up to 20% more observations to detect a

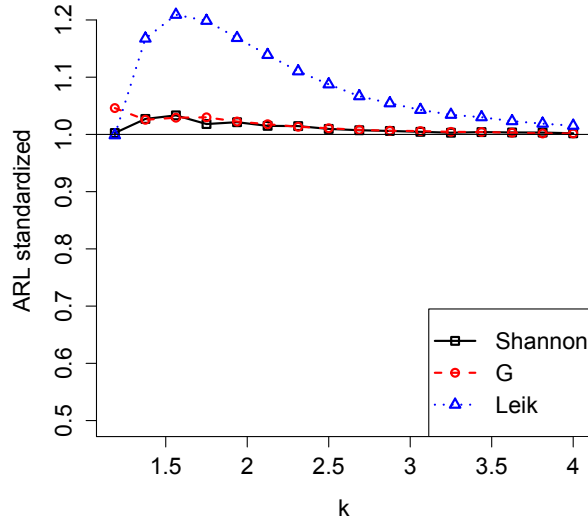


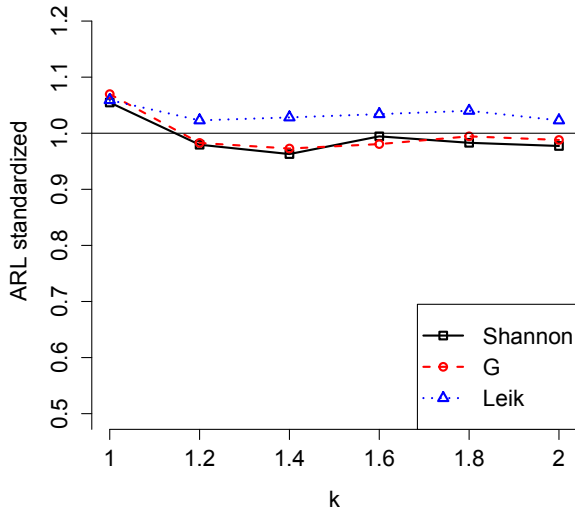
Figure 3:  $ARL$  of  $CPE_G$ ,  $CPE_S$ , and  $CPE_L$  for a standard Gaussian distribution where the standard deviations are multiplied by the shift-factor  $k$ . All  $ARL$ -values are reported as ratios compared to the  $ARL$ -value of the  $S$ -chart.

shift in the process' variance and is therefore not recommended for usage in this particular scenario.

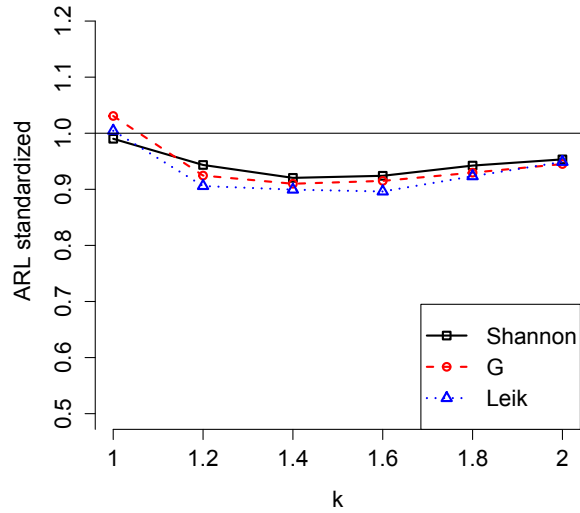
Nonetheless, we assume that there are situations, in which the Leik-chart outperforms every other control chart. For this purpose, we analyse the  $\phi$ -chart's behavior under several alternative families of distributions, which are summarized in table 1. Figure 4 compares the  $G$ -, Leik-, and Shannon-chart at a non-normal distribution of the production process. Again, all  $ARL$ -values are reported as ratio of the chart's  $ARL$  compared to the  $ARL$  of the  $S$ -chart. Three results can be derived by interpreting the ratio of the  $ARL$ -values. As first result, it seems that for heavy tail symmetric distributions (excess kurtosis of 6), deviations can be detected similarly by any of the applied procedures. If the process is e.g. from a Student  $t$  distribution with  $\nu = 5$ , extreme observations occur way more often as under a Gaussian distribution. In our simulation, the  $S$ -chart can detect such outliers very quickly, since an arbitrarily large value has an arbitrarily large effect on  $S$  which makes  $S$  very sensitive to outliers.

Nonetheless, in this scenario, the  $G$ -chart, as already discussed by [Riaz and Saghir \(2007\)](#), and the Shannon-chart perform similar to the regular  $S$ -chart. Merely the Leik-chart needs

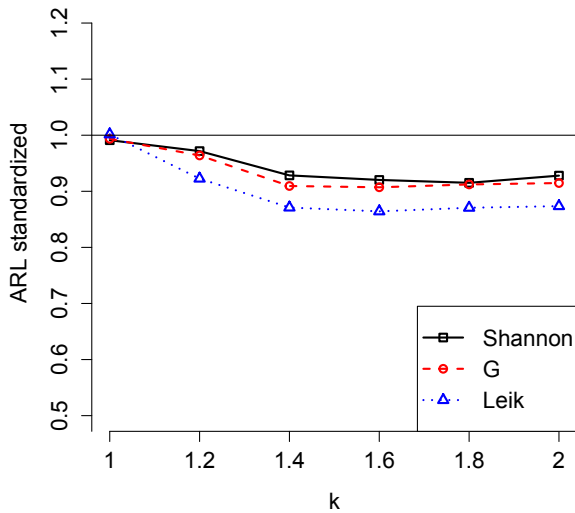
(a)  $ARL$ -ratios for samples from the Student  $t$  distribution with  $\nu = 5$ .



(b)  $ARL$ -ratios for samples from the standardized logistic distribution.



(c)  $ARL$ -ratios for samples from the standardized Laplace distribution.



(d)  $ARL$ -ratios for samples from the exponential distribution with  $\lambda = 1$ .

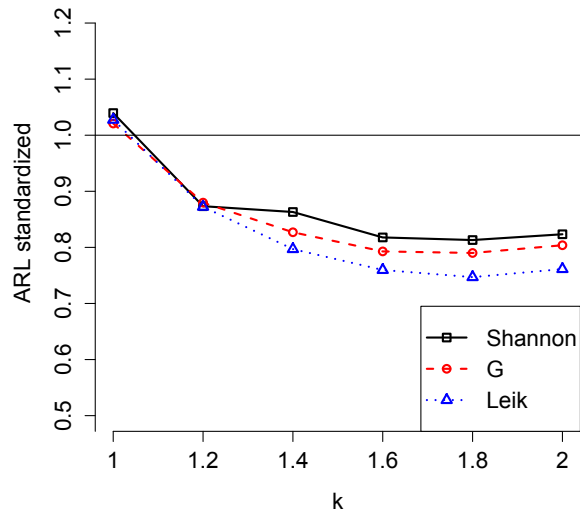


Figure 4:  $ARL$  of  $G$ -, Shannon-, and Leik-chart for the Student  $t$  (a), the logistic (b), the Laplace (c), and the exponential distribution (d). The standard deviations of each distribution are multiplied by the shift-factor  $k$  – the horizontal axis displays the shift of the applied distributions ( $k = 1$  refers to  $ARL_0$ ,  $k > 1$  to  $ARL_1$ ). All  $ARL$ -values are reported as ratios compared to the  $ARL$ -value of the  $S$ -chart.

about 5% more observations in order to detect an out-of-control process.

The second result is that at symmetric distributions with lighter tails than the  $t(5)$ -distribution<sup>6</sup>, all three charts ( $G$ -, Shannon-, Leik-chart) require less observations to detect an out-of-control process than the classical  $S$ -chart. Shannon- and  $G$ -chart perform similar, while both are dominated by the Leik-chart which requires the lowest amount of observations.

All the three analysed alternative distributions – Student  $t$ , logistic, and Laplace distribution – share one common feature: The larger the shift in variability, the more similar are Shannon-, Leik-, and  $G$ -charts to each other as well as they are to the  $S$ -chart. This convergence seems to be accelerated if the tails of the distribution are heavy.

The third result is that with increasing shift in the standard deviation at non-symmetric distributions (up to see figure 4 (d)), the better the improvement achieved by using the Leik-chart compared to any other chart (up to 25% less observations needed on average to detect an out-of-control process). However, for large shift values this improvement seems to vanish again as the ARL curve converges to 1 again.

The exponential distribution, used as non-symmetric distribution, is commonly used for modeling waiting time in production processes, see e.g. Qiu (2014). Therefore, we apply the Leik-chart in the next section to a more general family of distributions with a half-bounded domain that contains the exponential family and as a special case, the gamma distribution.

### 3.3. $\phi$ -charts for the gamma distribution

In some situations, especially when some kind of waiting time is involved in a production process, the quantity of interest follows a gamma distribution (c.f. Zhang et al. (2007)). The shape parameter  $\tau$  of a gamma distribution regulates the hazard rate – one can distinguish between

- $\tau < 1$  : monotonically decreasing hazard rate,
- $\tau = 1$  : constant hazard rate (exponential distribution),
- $\tau > 1$  : monotonically increasing hazard rate.

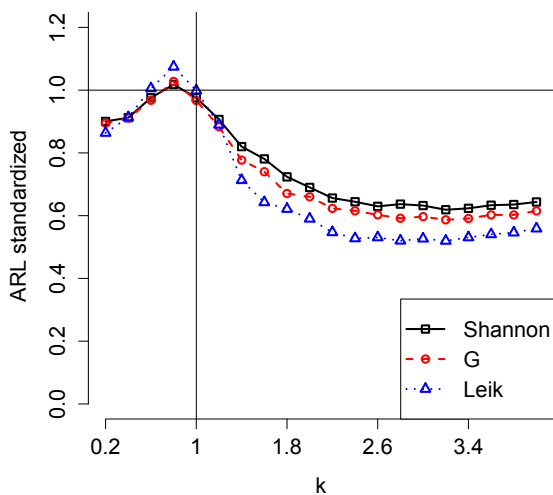
We showcase two parametrizations of the gamma distribution from table 1 covering both decreasing ( $\tau = 0.5$ , figure 5 (a)) as well as increasing ( $\tau = 2$ , figure 5 (b)) hazard rates.

---

<sup>6</sup>that is e.g. the logistic or the Laplace distribution.

As we can see in figure 5, in case of monotonically increasing as well as decreasing hazard rates the Leik-chart outperforms the  $S$ -chart by far in detecting out-of-control situations. The Leik-chart has an even lower value of the  $ARL_1$  than the  $G$ -chart or the Shannon-chart ( $k > 1$ ). It needs approximately 5-15% less observations to detect an out-of-control situation. All four control charts show a similar  $ARL_0$  value if the process' standard deviation lies in between its boundaries ( $k = 1$ ).

(a)  $ARL$ -ratios for samples from the gamma distribution with  $\tau = 0.5$ .



(b)  $ARL$ -ratios for samples from the gamma distribution with  $\tau = 2$ .

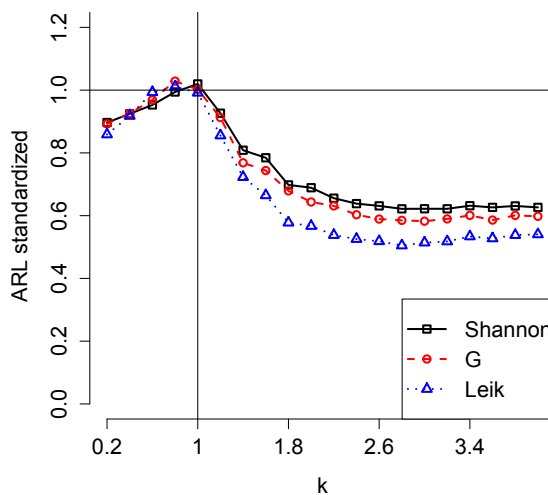


Figure 5:  $ARL$  ratios between Shannon-,  $G$ -, and Leik-chart compared to the  $S$ -chart when the population's distribution is a gamma distribution with shape parameter  $\tau = 0.5$  (a) and  $\tau = 2$  (b) for different shifts  $k$ .

This promising result encourages us to apply the new control charts to an actual data set from a refrigerator production process.

### 3.4. Application to real data

In this section, we evaluate the  $S$ -, Leik-, Shannon- and Gini-charts to a data set from Wild and Seber (2000), which contains the thickness of paint on refrigerators for a sample of size  $n = 5$  from 20 shifts of production. The first 15 shifts are set as training data and for the last 5 shifts (test data) a quality check is performed to determine whether or not the process is still under control. Table 2 lists all available data, normalized using the standard deviation from the first 15 shifts.

Table 2: Data set of the thickness of paint on refrigerators for a sample of size  $n = 5$  from 20 shifts of production. The data set has been split into a training set containing the first 15 shifts, and a test set containing the remaining 5 shifts. The sample data has been normalized using the standard deviation of the training data.

| Shift no.       | Samples              |         |         |         |         | Subgroup |        |        |        |         |         |
|-----------------|----------------------|---------|---------|---------|---------|----------|--------|--------|--------|---------|---------|
|                 | Normalized thickness |         |         |         |         | Mean     | $R$    | $S$    | $G$    | $CPE_S$ | $CPE_L$ |
| <b>Training</b> |                      |         |         |         |         |          |        |        |        |         |         |
| 1               | 9.3223               | 7.9412  | 8.9770  | 8.2865  | 9.3223  | 8.7699   | 1.3811 | 0.6272 | 0.7596 | 0.5881  | 0.9668  |
| 2               | 8.9770               | 8.2865  | 8.9770  | 7.9412  | 9.6676  | 8.7699   | 1.7263 | 0.6731 | 0.8286 | 0.6514  | 0.9668  |
| 3               | 7.9412               | 7.9412  | 8.2865  | 8.6317  | 8.2865  | 8.2174   | 0.6905 | 0.2889 | 0.3453 | 0.2701  | 0.4143  |
| 4               | 9.6676               | 7.9412  | 8.2865  | 8.9770  | 9.3223  | 8.8389   | 1.7263 | 0.7160 | 0.8977 | 0.6993  | 1.1049  |
| 5               | 8.9770               | 8.6317  | 8.9770  | 7.2507  | 9.6676  | 8.7008   | 2.4169 | 0.8937 | 1.0358 | 0.8258  | 1.1049  |
| 6               | 7.5959               | 7.9412  | 9.3223  | 7.5959  | 8.9770  | 8.2865   | 1.7263 | 0.8097 | 0.9668 | 0.7471  | 1.2430  |
| 7               | 7.5959               | 8.9770  | 8.2865  | 6.9054  | 7.9412  | 7.9412   | 2.0716 | 0.7720 | 0.9668 | 0.7626  | 1.1049  |
| 8               | 9.6676               | 8.9770  | 8.9770  | 9.3223  | 8.6317  | 9.1151   | 1.0358 | 0.3937 | 0.4834 | 0.3813  | 0.5524  |
| 9               | 8.2865               | 9.6676  | 8.2865  | 7.5959  | 7.9412  | 8.3555   | 2.0716 | 0.7873 | 0.8977 | 0.7147  | 0.9668  |
| 10              | 8.9770               | 7.9412  | 6.9054  | 8.6317  | 8.2865  | 8.1484   | 2.0716 | 0.7949 | 0.9668 | 0.7626  | 1.1049  |
| 11              | 10.7034              | 10.3581 | 12.0844 | 9.6676  | 10.3581 | 10.6343  | 2.4169 | 0.8937 | 1.0358 | 0.8258  | 1.1049  |
| 12              | 8.2865               | 9.6676  | 7.5959  | 10.0128 | 8.6317  | 8.8389   | 2.4169 | 0.9947 | 1.2430 | 0.9694  | 1.5192  |
| 13              | 7.2507               | 11.0486 | 8.6317  | 8.9770  | 9.6676  | 9.1151   | 3.7980 | 1.3940 | 1.7263 | 1.3661  | 1.9335  |
| 14              | 7.5959               | 9.6676  | 7.2507  | 7.5959  | 8.2865  | 8.0793   | 2.4169 | 0.9643 | 1.1049 | 0.8737  | 1.2430  |
| 15              | 8.2865               | 10.3581 | 8.6317  | 8.6317  | 6.9054  | 8.5627   | 3.4527 | 1.2304 | 1.4501 | 1.1592  | 1.5192  |
| <b>Test</b>     |                      |         |         |         |         |          |        |        |        |         |         |
| 16              | 10.7034              | 8.9770  | 8.9770  | 9.6676  | 7.2507  | 9.1151   | 3.4527 | 1.2592 | 1.5192 | 1.2071  | 1.6573  |
| 17              | 10.0128              | 8.2865  | 10.0128 | 4.4885  | 6.2149  | 7.8031   | 5.5243 | 2.4243 | 2.9693 | 2.3047  | 3.7289  |
| 18              | 6.5601               | 5.5243  | 8.9770  | 11.3939 | 11.3939 | 8.7699   | 5.8696 | 2.7033 | 3.3146 | 2.5595  | 4.2813  |
| 19              | 7.9412               | 8.9770  | 9.3223  | 9.6676  | 11.0486 | 9.3913   | 3.1074 | 1.1294 | 1.3811 | 1.0960  | 1.5192  |
| 20              | 6.2149               | 9.6676  | 7.9412  | 6.9054  | 10.0128 | 8.1484   | 3.7980 | 1.6666 | 2.0716 | 1.6054  | 2.6241  |

A goodness of fit test for the first 75 observations results in p-values of 0.4112 for the gamma and 0.3073 for the Gaussian distribution. Therefore we use the gamma distribution for determining the critical values of the control charts. Maximum likelihood estimation leads to parameters  $\tau = 78.8544$  and  $\theta = 0.1102$ . After the training set, the control charts are initialized using simulated UCL and LCL based on 1,000,000 samples of size  $n = 5$  at a level of 0.5%. Figure 6 lists the four resulting processes and the application to the 5 test shifts.

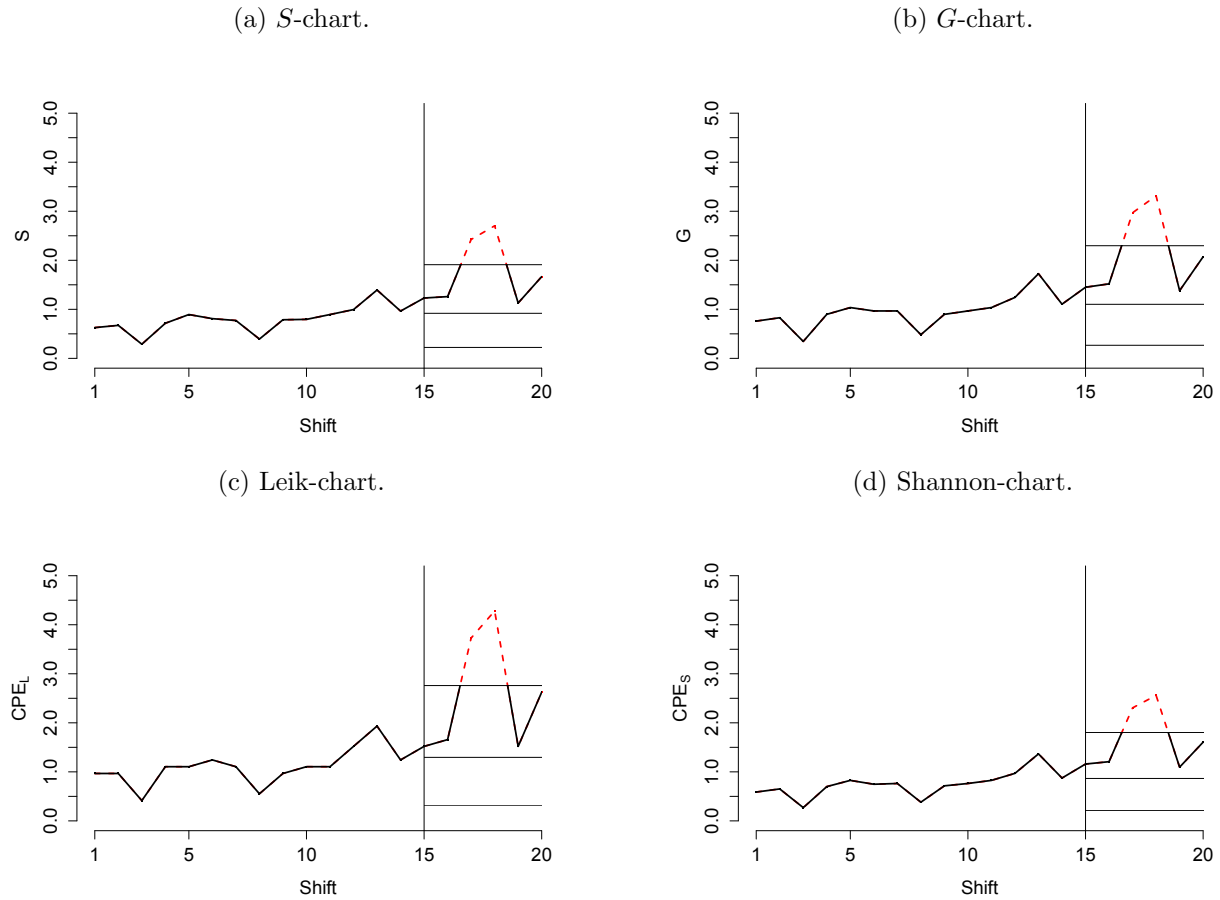


Figure 6:  $S$ -,  $G$ -, Leik-, and Shannon-chart of the data set from table 2. The first 15 shifts have been used to calibrate the control chart by estimating LCL and UCL. The charts are applied to the last 5 test shifts. Horizontal lines denote the UCL, the mean of the process, and LCL (top down). Red dashed line indicates an out-of-control situation.

Clearly, all four control charts detect an out-of-control situation in the shifts 17 and 18,

which would in practice result in a termination of the production process. To strengthen the results from the Monte Carlo simulations of the previous sections however, more data would be required together with the information if the process has been out-of-control or not.

#### 4. Conclusions

This paper introduced a general class of entropy based control charts, the  $\phi$ -charts. We analysed the performance of  $\phi$ -charts at monitoring the variance of production processes compared to other established Shewhart control charts.

Our results showed, that the wide class of  $\alpha$ -charts, containing the well known  $G$ -chart as a special case for  $\alpha = 2$  as well as the Shannon-chart as a limiting case for  $\alpha \rightarrow 1$ , does not provide any improvement over the classical Shewhart control charts for values of  $\alpha \neq 2$ . The  $ARL$  of  $\alpha$ -charts is very similar to the  $ARL$  of the  $G$ -chart in the analyzed scenarios. One reason for this finding could be the almost equally shaped kernel functions of the underlying  $CPE_\alpha$ , which weight observations in a similar manner.

However, we discovered that the usage of Leik control charts can be advantageous compared to established Shewhart control charts if the underlying process follows an exponential, Laplacian, or gamma distributed law. Leik control charts are found to outperform both the classical  $S$ -chart and the  $G$ -chart if the variability of the process is out-of-control. Further research should apply this Leik-chart to actual data from production processes following a gamma distribution and investigate the economically advantageous implications of using this new  $\phi$ -chart compared to using a classical Shewhart control chart.

Furthermore, for processes which follow a distribution with domain  $\mathbb{R}^+$  the analysis of the performance of a control chart, that is based on the cumulative residual entropy (as in [Wang et al. \(2003\)](#)), could be of interest for further research.

#### Bibliography

- Burbea, J., Rao, C., 1982. On the convexity of higher order Jensen differences based on entropy functions (Corresp.). *IEEE Transactions on Information Theory* 28 (6), 961–963.
- Burr, I. W., 1967. The effect of non-normality on constants for  $\bar{x}$  and  $R$  charts. *Industrial Quality Control* 23 (11), 563–569.



- Chan, L. K., Hapuarachchi, K. P., Macpherson, B. D., 1988. Robustness of mean  $E(X)$  and R charts. *IEEE Transactions on Reliability* 37 (1), 117–123.
- Crowder, S. V., 1987. A simple method for studying run – length distributions of exponentially weighted moving average charts. *Technometrics* 29 (4), 401–407.
- David, H. A., 1968. Gini’s mean difference rediscovered. *Biometrika* 55 (3), 573–575.
- de Luca, A., Termini, S., 1972. A definition of a nonprobabilistic entropy in the setting of fuzzy sets theory. *Information and Control* 20 (4), 301–312.
- Ebrahimi, N., 1996. How to measure uncertainty in the residual life time distribution. *Sankhya: The Indian Journal of Statistics, Series A* 58 (1), 48–56.
- Ewan, W. D., 1963. When and how to use cu-sum charts. *Technometrics* 5 (1), 1–22.
- Havrda, J., Charvát, F., 1967. Quantification method of classification processes. concept of structural  $\alpha$ -entropy. *Kybernetika* 3 (1), 30–35.
- Klein, I., Mangold, B., Doll, M., 2016. Cumulative paired  $\phi$ -entropy. *Entropy* 18 (7), 248.  
URL <http://www.mdpi.com/1099-4300/18/7/248>
- Leik, R. K., 1966. A measure of ordinal consensus. *The Pacific Sociological Review* 9 (2), 85–90.
- Liu, B., 2015. *Uncertainty Theory*. Springer-Verlag, Berlin/Heidelberg, Germany.
- Page, E. S., 1954. Continuous inspection schemes. *Biometrika* 41 (1/2), 100–115.
- Qiu, P., 2014. *Introduction to Statistical Process Control*. Chapman & Hall/CRC texts in statistical science series. CRC Press, Boca Raton, USA.
- Riaz, M., Saghir, A., 2007. Monitoring process variability using Gini’s mean difference. *Quality Technology & Quantitative Management* 4 (4), 439–454.
- Saghir, A., Lin, Z., 2015. Designing of Gini-chart for exponential, t, logistic and Laplace distributions. *Communications in Statistics – Simulation and Computation* 44 (9), 2387–2409.

- Shewhart, W. A., 1931. Economic Control of Quality of Manufactured Product. D. Van Nostrand Company Inc, New York, USA.
- Wang, F., Vemuri, B. C., Rao, M., Chen, Y., 2003. A new & robust information theoretic measure and its application to image alignment. In: Taylor, C., Noble, J. A. (Eds.), Information processing in medical imaging. Vol. 2732 of Lecture notes in computer science. Springer-Verlag, Berlin and New York, pp. 388–400.
- Wild, C. J., Seber, G. A. F., 2000. Chance Encounters: A First Course in Data Analysis and Inference. John Wiley, New York, USA.
- Zhang, C. W., Xie, M., Liu, J. Y., Goh, T. N., 2007. A control chart for the gamma distribution as a model of time between events. International Journal of Production Research 45 (23), 5649–5666.